Bulletin of the Earthquake
Research Institute
University of Tokyo
Vol. 65 (1990) pp. 541-569

Fault Heterogeneity of Inland Earthquakes in Japan

Minoru TAKEO

Earthquake Research Institute

and

Naoya MIKAMI

Matsushiro Seismological Observatory, Japan Meteorological Agency

(Received June 27, 1990)

Abstract

Detailed rupture processes of six intraplate earthquakes in Japan, the 1961 Kitamino earthquake, the 1969 GifuKen-Chubu earthquake, the 1974 Izu-Hanto-Oki earthquake, the 1975 OitaKen-Chubu earthquake, the 1980 Izu-Hanto-Toho-Oki earthquake, and the 1984 NaganoKen-Seibu earthquake, are compiled and compared to each other to make clear common features of an earthquake rupture process. The rupture processes are obtained by waveform inversion using strong motion seismograms in previous studies. Five of these rupture processes are also compared with distributions of precisely determined aftershocks.

Earthquakes with relatively smooth rupture propagation, such as the 1974 Izu-Hanto-Oki earthquake and the 1961 Kitamino earthquake, represent smoother slip distribution than earthquakes with relatively irregular rupture propagation, such as the 1969 GifuKen-Chubu earthquake and the 1980 Izu-Hanto-Toho-Oki earthquake. It is also recognized that aftershocks of magnitude greater than 4 do not occur in the large slip area. Most large aftershocks take place near the edge of the large slip region and in the small slip region. Aftershocks also tend to cluster near the edge of the large slip region. These results are very consistent with numerical experiments of dynamic rupture, so it is suggested that the relation between aftershocks and coseismic slip pattern obtained in this paper hold generally for earthquake rupture processes.

A clear delay of rupture propagation occurs in the large slip area during the 1969 GifuKen-Chubu earthquake: on the other hand, the small slip area in the 1980 Izu-Hanto-Toho-Oki earthquake is character-

ized by a deceleration of rupture propagation. The large slip area in the former case is interpreted as a barrier which resisted fracturing at first and was broken with a high stress drop. In the latter case, mechanical weakness due to volcanic structure located around the source region, seems to have affected the rupture process. A similar geological condition may have affected the rupture process of the 1978 Izu-Oshima-Kinkai earthquake which occurred about 10 km south of the 1980 Izu-Hanto-Toho-Oki earthquake.

1. Introduction

During the last decade, waveform inversion analyses have revealed the spatial and temporal distribution of slip over fault areas where earthquakes occur, using strong motion seismograms as well as teleseismic seismograms (*e.g.*, HARTZELL and HEATON, 1983; MORI and SHIMAZAKI, 1985; KIKUCHI and FUKAO, 1985; TAKEO and MIKAMI, 1987; FUKUYAMA and IRIKURA, 1986; TAKEO, 1988, 1989). The complicated rupture processes must be related to the inhomogeneous strength, friction and initial stress (prestress) on the fault. Few attempts have been made to compare the spatial and temporal distributions of slip with other geophysical observations such as the corresponding distribution of aftershocks (*e.g.* DOSER and KANAMORI, 1986; MENDOZA and HARTZELL, 1988; FUKUYAMA, 1990). DOSER and KANAMORI (1986) found that the aftershock activity of the 1979 Imperial Valley earthquake occurred outside of the large slip region. MENDOZA and HARTZELL (1988) compared aftershock patterns following five inland earthquakes in North America to the corresponding distributions of coseismic slip obtained from previous analyses of the strong motion and teleseismic waveforms. They pointed out that aftershocks occurred mostly outside of or near the edges of the source areas indicated by the patterns of coseismic slip. FUKUYAMA (1990) compared rupture processes of three earthquakes in Japan with the distribution of aftershocks, and pointed out that the large seismic moment release during the main events suggested low aftershock activity. He also related rupture propagation to discontinuities in geological structures, stress drop to aftershock expansions.

In this paper, we compile the results on rupture processes of six intraplate earthquakes in Japan obtained from waveform inversion analyses using displacement type strong motion seismograms. Fig. 1 shows epicenters of very shallow earthquakes of magnitude equal to or greater than 6.4 from 1961 to 1985. Solid circles indicate earthquakes compiled in this paper: the 1961 Kitamino earthquake (MIKAMI and TAKEO, 1987), the 1960

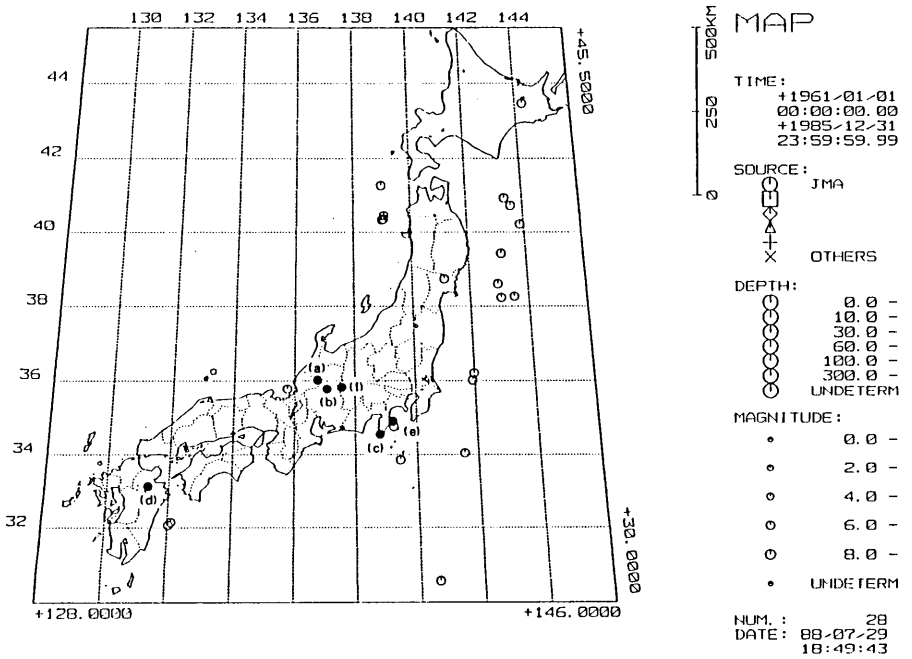

Fig. 1. Epicenters of very shallow earthquakes of magnitudes equal to or greater than 6.4, which occurred from 1961 to 1985. These source depths are shallower than 30 km. Six solid circles indicate earthquakes compiled in this paper. These are the Kitamino earthquake of 1961 (a), the GifuKen-Chubu earthquake of 1969 (b), the Izu-Hanto-Oki earthquake of 1974 (c), the OitaKen-Chubu earthguake of 1975 (d), the Izu-Hanto-Toho-Oki earthquake of 1980 (e), and the Nagano Ken-Seibu earthquake of 1984 (f). This map was written by the SEIS routine of Earthquake Research Institute, Earthquake Prediction Data Center (EPDC).

GifuKen-Chubu earthquake (MIKAMI and TAKEO, 1990), the 1974 Izu-Hanto-Oki earthquake (TAKEO, 1989), the 1975 OitaKen-Chubu earthquake (HATANAKA and TAKEO, 1989), the Izu-Hanto-Toho-Oki earthquake (TAKEO, 1988), and the 1984 NaganoKen-Seibu earthquake (TAKEO and MIKAMI, 1987). The five spatial distributions of slip on the fault are compared with these aftershock patterns, and the rupture processes are compared to each other. The results of these comparisons show some common characteristics of the earthquake rupture process.

2. Analysis method and Data

The rupture processes of six earthquakes summarized in this paper were obtained using waveform inversion method by TAKEO (1987). This method is simply outlined as follows.

A rectangular fault is discretized into subfaults which start rupturing with arbitrary magnitudes at arbitrary times. Each subfault has an assumed orientation and rupture duration. The *i-th* component of the synthetic seismogram at a particular station is given by the summation of weighted Green's functions,

$$u_i(t\,;\,m_j, t_j^s)=\sum_j m_j w_{ij}(t\,;\,t_j^s)\,,$$

where m_j and t_j^s denote the seismic moment and the starting time of rupture at the *j-th* subfault, respectively. w_{ij} is the Green's function which represents the *i-th* component of seismograms excited by the rupture on the *j-th* subfault. For each subfault, w_{ij} is first calculated for a point source and then convolved with a parabolic ramp function. We assume that the rise time of the ramp function corresponds to the rupture duration for the subfault. Directivity associated with rupture propagation on the whole fault plane is automatically included in the synthetic seismogram because u_i is calculated by summation of the Green's functions which are subject to the time shifts, t_j^s.

The observed seismograms are digitized at a time step of Δt; then, the *i-th* component of observations ($O_i(t)$) is expressed as a discrete time series $O_i(t_l)$, $l=1, N_i$, where N_i is the total number of points for the *i-th* component. The synthetic seismogram is calculated at the same sampling interval and is expressed as $u_i(t_l)$. Then, m_j and t_j^s are determined by minimizing a squared error $S(m_j, t_j^s)$, defined by

$$S(m_j, t_j^s)=\sum_{i,l}[O_i(t_l)-u_i(t_l\,;\,m_j, t_j^s)]^2\,.$$

To solve this problem, we employ the Householder technique and the modified Marquardt technique for linear and nonlinear inversion algorithm, respectively. The Green's functions are calculated by the use of reflection-transmission matrices (*e.g.*, KENNETT and KERRY, 1979) and the discrete wavenumber method (BOUCHON, 1980), assuming an anelastic structure (*e.g.*, TAKEO, 1985), or by the DWFE method (OLSON, 1982).

Our model assumes that each subfault has a fixed slip orientation, a fixed fault plane geometry, and a fixed rupture duration. If these assumed values are not suitable to represent a practical rupture process, negative seismic moments and/or irregular rupture propagation are obtained from inversion even though the error is reduced. For such a case, it is necessary to review the model. It is a fundamental assumption in our analyses that the rupture process does not fluctuate over a fault plane, so if there are several solutions which show equally small residuals, the solution having

the smoothest rupture process is taken as the best solution.

Seismograms recorded by Japan Meteorological Agency (JMA) strong motion seismographs were used in the analyses of the detailed rupture processes compiled in this paper. All JMA seismographs used are mechanical, and the instrumental constants are: T_0 (pendulum period)=6 sec for the horizontal component and T_0=5 sec for the vertical component; ε (damping ratio)=8; and v (magnification)=1. Correcting the distortion of the original records due to the mechanism of the recording system, we digitized the records at a rate of 4 samples/sec except for the records of the 1974 Izu-Hanto-Oki earthquake, which were digitized at a rate of 2 samples/sec. The rupture process of each subfault was approximated with a point source in our model, so waves with periods shorter than the point source duration could not be analyzed. The digitized seismograms were filtered using a low-pass Chebyshev filter. Individual papers in which the rupture process of each earthquake is analyzed are referred to for the filter's parameters and the velocity structures used in the calculation of the Green's function.

3. Rupture Process

3.1. The 1980 Izu-Hanto-Toho-Oki earthquake

The Izu-Hanto-Toho-Oki earthquake occurred off east of Izu Peninsula on June 29, 1980. Fig. 2 shows the location of the JMA strong motion seismographs in and around the Izu Peninsula. Records obtained at Ajiro (AJI), Oshima (OSH), Mishima (MIS), Irozaki (NGT), Tateyama (TAT), and Shizuoka (SHZ) were utilized for the inversion analysis of the rupture process (Takeo, 1988). This earthquake involves left-lateral strikeslip motion on the almost vertical fault with a strike of N10°W. The fault is estimated to be 20 km long and 12 km wide from the distribution of aftershocks relocated by MATSU'URA (1983). The fault plane was divided into twenty 4 km (length)×3 km (width) subfaults. The subfault arrangement is shown in Fig. 3 with the aftershock pattern following the main event. The seismic moments and the starting time of rupture at each subfault were determined by minimizing the equared error between observed and synthetic seismograms, assuming the source duration of each subfault to be 3 sec.

The distribution of coseismic slip converted from the seismic moment (m_j) on each subfault and the rupture fronts at every second inferred from the values of t_j^s are shown in Fig. 17 with rupture processes of five other earthquakes. The observed seismograms are compared to the synthetic seismograms in Fig. 4. It is obvious that the fit of the synthetics to the

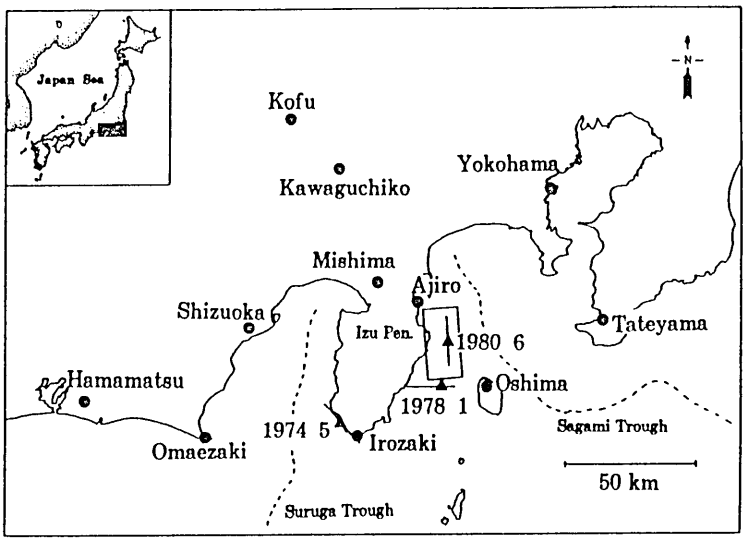

Fig. 2. Distribution of stations (circles) and epicenters of the 1974 Izu-Hanto-Oki earthquake, the 1978 Izu-Oshima-Kinkai earthquake, and the 1980 Izu-Hanto-Toho-Oki earthquake (triangles). The Izu-Hanto-Toho-Oki earthquake occurred at 1620JST (Japan Standard Time) on June 29, 1980. Solid lines illustrate the horizontal projection of fault planes of these three earthquakes. The area closed by a rectangle shows the region represented in Fig. 3 [after TAKEO (1988)].

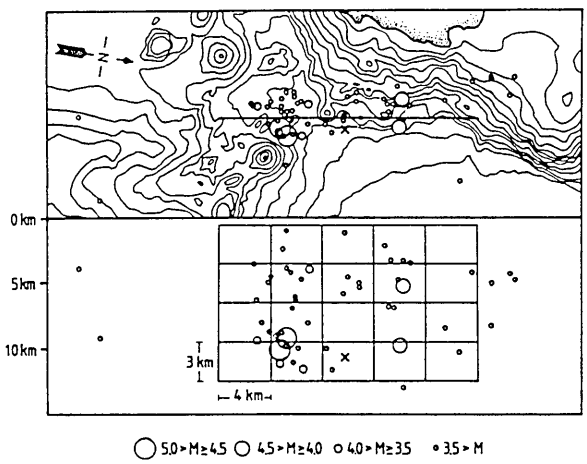

Fig. 3. Example of subfault arrangement. Aftershocks occurring in the first 32 hours after the main event are also represented by open circles. A small cross indicates the hypocenter of the main event. Tne solid line in the map shows the horizontal fault line projection at a depth of 5 km. Contours on the map represent the submarine topography (HYDROGRAPHIC DEPARTMENT, 1977) and are drawn every 100 m. The vertical section is in the N10°W direction [after TAKEO (1988)].

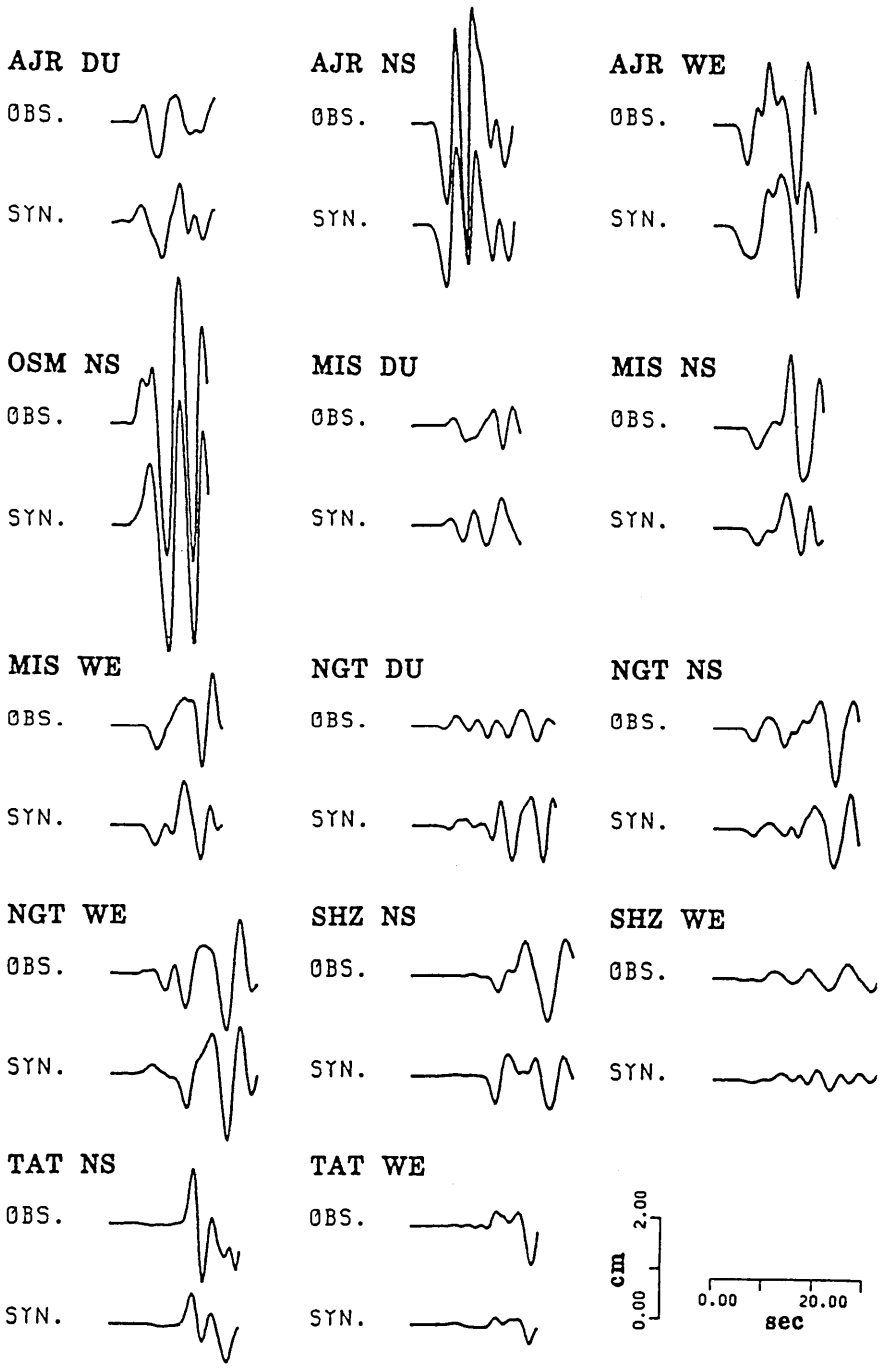

Fig. 4. Comparison of observed seismograms with synthetic seismograms obtained by using the solution for the 1980 Izu-Hanto-Toho-Oki earthquake [after TAKEO (1988)].

observations is good. Details of the analysis procedure are given in TAKEO (1988).

Large slip occurs in the deeper part of the fault, especially near the hypocenter, and at the southern end of the fault. The maximum slip amounts to 2.7 m and the average slip on the whole fault is 1.1 m. The rupture propagates southward from the central part of the fault and spreads to the shallow area of the northern part after a delay of about 5 sec after the initiation of the event. The total seismic moment is 7×10^{25} dyne·cm (TAKEO, 1988).

3.2. The 1974 Izu-Hanto-Oki earthquake

The Izu-Hanto-Oki earthquake occurred near the southern tip of the Izu Peninsula on May 9, 1974 (see Fig. 2). This earthquake represents right-lateral strike-slip motion on the almost vertical fault with a strike of N45°W. Horizontal components of seismograms recorded at Tateyama (TAT), Yokohama (YOK), Mishima (MIS), Kawaguchiko (FUN), Kofu (KOF), Shizuoka (SHZ), and Hamamatsu (HMM) were used for the inversion analysis. Based on the distribution of aftershocks (KARAKAMA *et al.*, 1974; ISHIBASHI *et al.*, 1975), the fault plane is estimated to be 25 km long and 9 km wide. The fault plane was divided into fifteen subfaults of 5 km (length) $\times$3 km (width) whose rupture durations were 3 sec.

In Fig. 18, coseismic slip of this earthquake inferred from the inver-

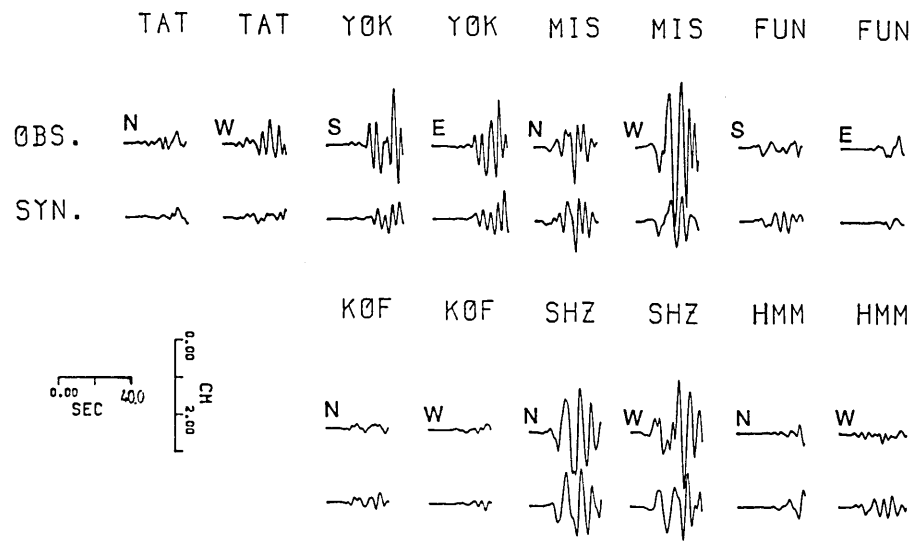

Fig. 5. Comparison of observed seismograms with synthetic seismograms obtained by using the solution for the 1974 Izu-Hanto-Oki earthquake [after TAKEO (1989)].

sion solution is contoured at 1 m intervals with the aftershock activity determined by a temporary seismic network which was installed in and around the source region several days after the main event. Small dots indicate hypocenters of aftershocks occurring from 1300JST on May 16 to 1200JST on May 18 (ISHIBASHI *et al.*, 1975). The rupture fronts at every second inferred from the inversion solution are shown in Fig. 17. In Fig. 5, the observed seismograms are compared to the synthetics calculated for the solution. For details of the analysis, see TAKEO (1989).

The rupture initiates at the central deeper part of the fault and bilaterally propagates to both sides smoothly. A slip larger than 1 m occurs from 3 km to 10 km in depth; its horizontal span is about 20 km around the hypocenter. Except for the southeastern end of the fault, slip smaller than 0.5 m occurs in the shallower region of the fault. The average slip over the whole fault is 1.0 m, and the total seismic moment is 7.6×10^{25} dyne·cm.

Surface fractures, associated with this earthquake, appeared in the source region along some of the fault lines trending northwest, and displayed right-lateral strike-slips. The major surface break is about 5.5 km long and slipped 0.45 m right-laterally with an 0.25 m upthrow relative to the NE side at the most (MATSUDA and YAMASHINA, 1974). The fault displacements along the major surface break are compared with the slips obtained from the inversion analysis. Horizontal solid lines in Fig. 6 represent the horizontal and vertical slips at the shallowest subfaults just beneath the surface break, and vertical lines in Fig. 6 indicate the observed fault displacements. The slip distribution obtained from seismograms is consistent with fault displacements along the surface break. Numerical experiments of dynamic fault rupture assuming uniform frictional strength and initial shear stress on the fault show that the fault slip increases gradually toward the ground surface when the rupture breaks the ground surface (*e.g.*, MIKUMO *et al.*, 1987). The fault slip of the 1974 Izu-Hanto-Oki earthquake, however, was concentrated in the deeper part of the fault. This does not agree with the result of numerical experiments. It is suggested that the shallower part of the fault has weaker frictional strength and/or lower initial shear stress than the deeper part of the fault.

3.3. The 1984 NaganoKen-Seibu earthquake

The NaganoKen-Seibu earthquake, accompanied with a large-scale landslide, occurred in the western part of Nagano Prefecture on September 14, 1984. The station distribution and epicenter are shown in Fig. 7 with the

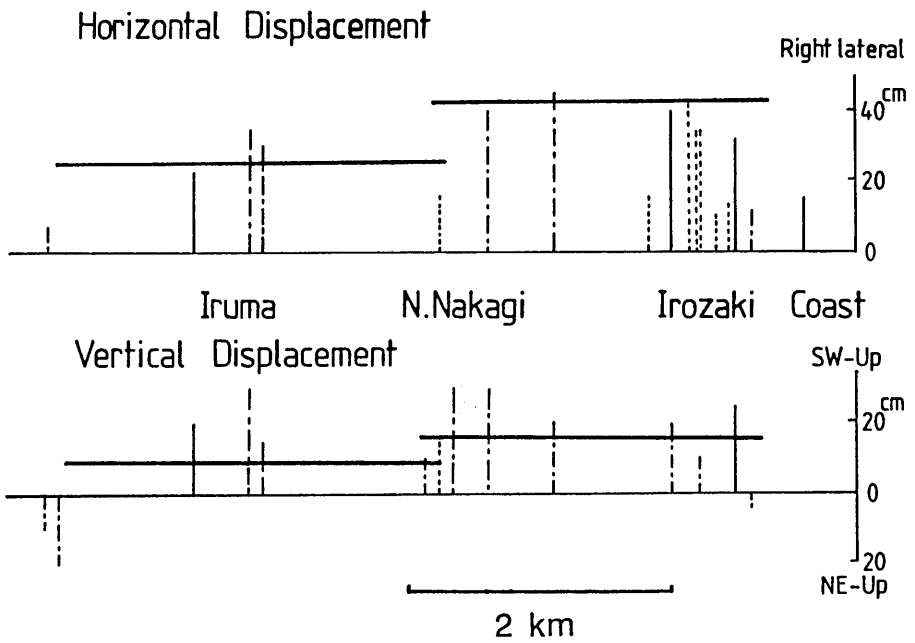

Fig. 6. Comparison of the slip inferred from the seismogram inversion with fault displacements along the surface fractures associated with this earthquake. Horizontal solid lines represent the horizontal and vertical slips at the shallowest subfaults just beneath the surface fractures. Vertical solid lines indicate displacement values measured directly on surface fractures in Tertiary rocks. Vertical chain lines denote values measured on or in the soil. Vertical dotted lines show values on construction such as a paved road [after TAKEO (1989)].

focal mechanism of this event. Records at Iida (IID), Takayama (TKY), Matsumoto (MTM), Gifu (GIF), and Matsushiro (MAT) were utilized for the inversion analysis. The nodal plane striking in the direction of N70°E agrees well with the strike of the distribution of aftershocks. The fault plane is estimated to be 12 km long and 9 km wide from the spatial distribution of aftershocks which occurred within the first 3 hours after the main event. The fault plane was divided into twelve 3 km (length)×3 km (width) subfaults whose rupture durations were 1.5 sec.

In Fig. 17, the distribution of coseismic slip and the rupture fronts at every second are shown. The hypocenter of the largest aftershock and the aftershocks which occurred before the largest aftershock (JAPAN MEIEOROLOGICAL AGENCY, 1986) are projected on the fault plane with the slip pattern (Fig. 18). In Fig. 8, the observed seismograms are compared to the synthetics calculated for the inversion solution. For details on the analysis see TAKEO and MIKAMI (1987).

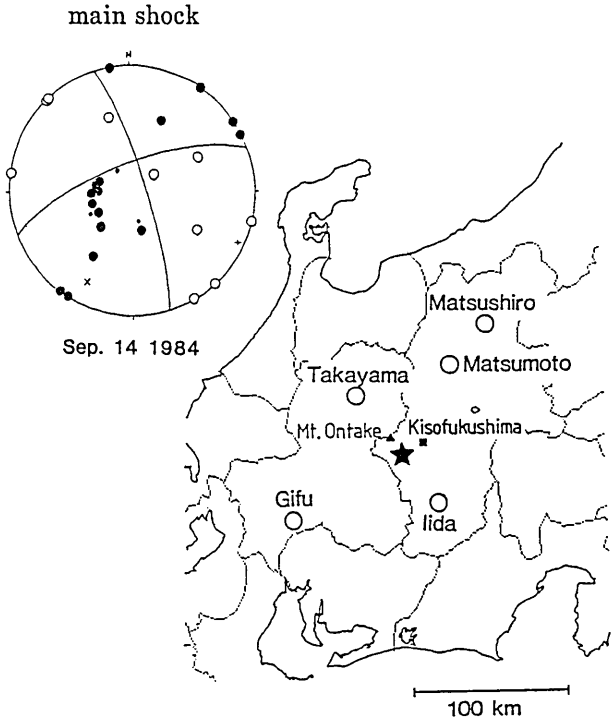

Fig. 7. Location of the Nagano-Ken-Seibu earthquake which occurred at 0848JST on September 14, 1984 (star) and locations of stations (open circles). The focal mechanism of this event is also shown in this figure. Solid and open circles in the focal mechanism indicate compressional and dilatational initial motions, respectively.

The rupture started at the central shallower part of the fault, and propagated over the whole fault within several seconds. A large slip, which amounts to 1.5 m–2.0 m, occurred in the near surface region; the slip seems to have been small on the deeper part of the fault. In particulr, no slip occurred at the deepest part of the western edge of the fault; nearby, the largest aftershock occurred. The total seismic moment was 4×10^{25} dyne·cm, and the maximum slip was 2 m.

3.4. The 1969 GifuKen-Chubu earthquake

The GifuKen-Chubu earthquake took place in the central part of Gifu Prefecture on September 9, 1969: the epicenter was about 40 km west of the epicenter of the 1984 NaganoKen-Seibu earthquake. This earthquake involved right-lateral strike-slip motion on an almost vertical fault with a strike of N27°W. Horizontal components of seismograms recorded at eight stations in Fig. 9 were used for the inversion analysis. These stations

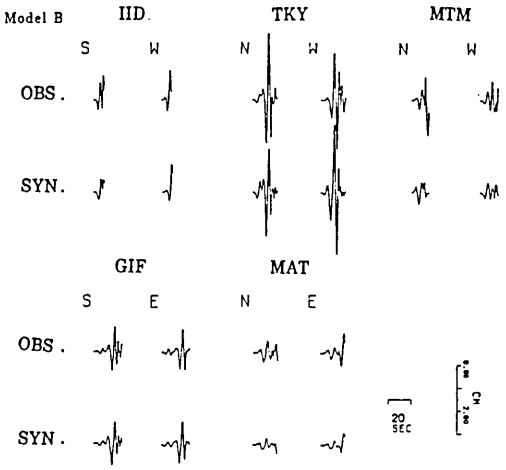

Fig. 8. Comparison of the observed seismograms at IID, TKY, GIF and MAT with synthetic seismograms obtained by using the solution for model B [after TAKEO and MIKAMI (1987)].

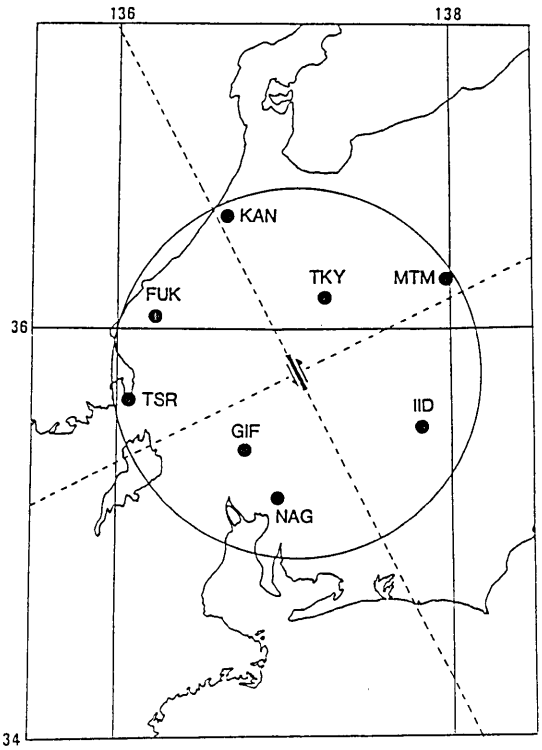

Fig. 9. Distribution of stations (solid circles) and the fault of the GifuKen-Chubu earthquake which occurred at 1415JST on September 9, 1969. The radius of the large open circle is 100 km; the center is located at the epicenter of this event.

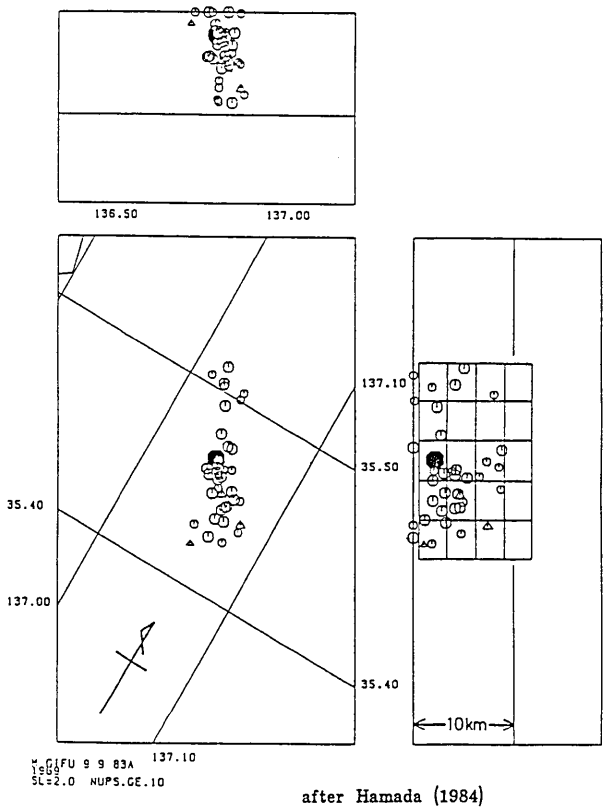

Fig. 10. The subfault arrangement used in this analysis. Aftershocks occurring in the first month after the main event are represented by open circles. The magnitudes of aftershocks are greater than 3.5. Locations were redetermined by HAMADA (1984). A solid circle indicates the hypocenter of the main event.

enclose the epicenter, and the epicentral distances are shorter than 100 km. Locations of precisely determined aftershocks of magnitude greater than 3.5, which occurred in the first month after the main event (HAMNDA, 1984), are shown in Fig. 10 with the subfaults arrangement employed in the analysis. The fault plane whose length and width were 20 km and 11.2 km, respectively, was divided into twenty 4 km (length)×2.8 km (width) subfaults. A rupture duration of 3 sec was assumed for each subfalt. Fig. 11 shows the comparison of observed seismograms with synthetic seismograms which were calculated using the inversion solution. It is obvious that a fit of the synthetics to the observations is good. The average slips on each subfault is shown in Table 1. The rupture fronts at every second in Fig. 17 were inferred from the starting times of rupture at

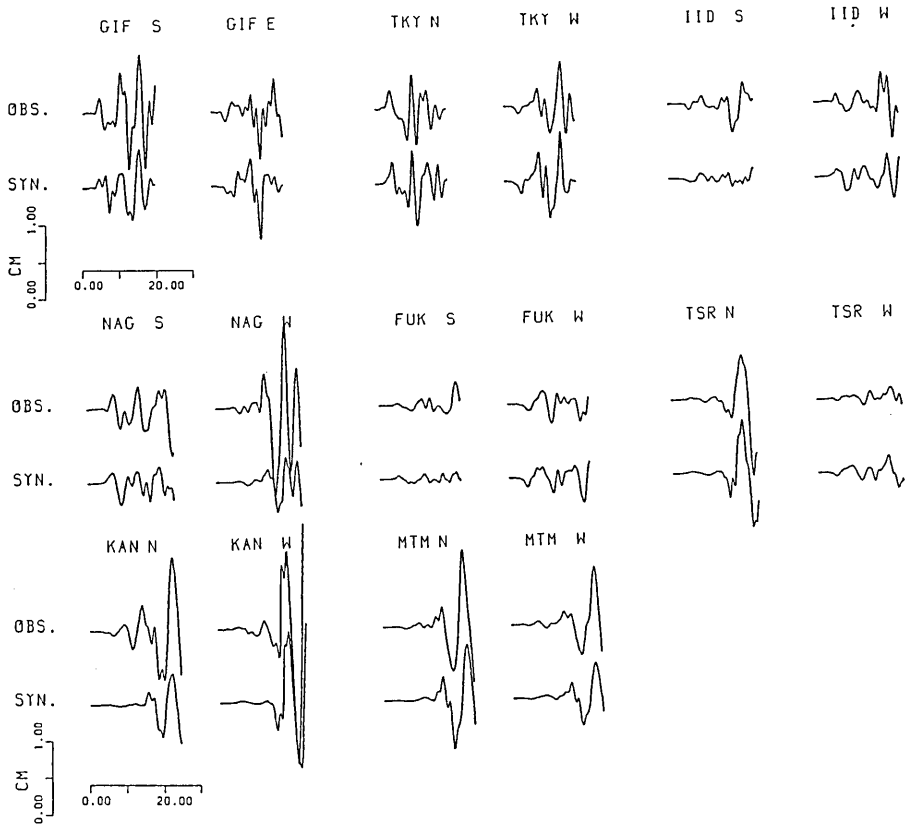

Fig. 11. Comparison of observed seismograms with synthetic seismograms obtained using the solution for the 1969 GifuKen-Chubu earthquake.

each subfault shown in Table 1. In Fig. 18, the coseismic slip is contoured at 0.5 m intervals with the distribution of aftershocks.

The rupture was initiated at the central shallower part of the fault, as in the 1984 NaganoKen-Seibu earthquake, and spreaded both directions with a slightly irregular pattern. The largest slip, 1.7 m, occurred at the northwest of and below the hypocenter; slip smaller than 0.4 m occurred on the shallowest part of the fault. The average slip over the whole fault was 0.68 m, and the total seismic moment was 5.4×10^{25} dyne·cm. MIKUMO (1973) analyzed seismic and geodetic data of this earthquake, and found that slips over the northwestern part of the fault might be considerably larger than the average slip of 0.6-0.7 m. Our rupture process is very consistent with Mikumo's result.

3.5. The 1961 Kitamino earthquake

A large earthquake of magnitude 7.0 occurred in the border region of Gifu, Fukui, and Ishikawa Prefectures on August 19, 1961. The epicenter was about 40 km northwest of the epicenter of the 1969 GifuKen-Chubu earthquake. The focal mechanism of this earthquake determined from the P-wave first motions are shown in Fig. 12 with locations of the hypocenter and stations used in the analysis. KAWASAKI (1975) analyzed this earthquake based on seismological and geographical data, and found that this event is a result of right-lateral reverse faulting on a fault plane with a length of 12 km and width of 10 km. HAMADA, (1984) relocated the aftershocks, and found a spatial extent of about 20 km southwest from the epicenter. Based on Kawasaki's and Hamada's results, we assumed a fault plane with a strike of N20°E and dip of 60° whose length and width were 16 km and 12 km, respectively. The epicenter was located at the northeastern end of the fault. The fault was divided into twelve 4 km (length)

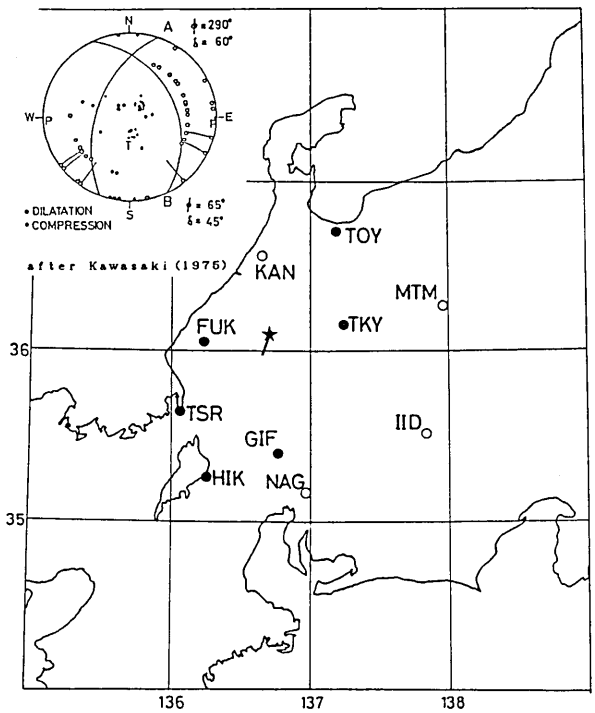

Fig. 12. Location of the Kitamino earthquake which occurred at 1433JST on August 19, 1961 (star) and locations of stations (solid circles). The focal mechanism of this event is also shown in this figure. Solid and open circles in the focal mechanism indicate compressional and dilatational initial motions, respectively.

×4 km (width) subfaults assuming a source duration for each subfault of 3 sec. Apparent in Fig. 13 is a good fit of the synthetic seismograms calculated for an inversion solution shown in Fig. 17 to the observed seismograms.

The rupture started at the northeastern end of the fault, and progressed southwestward smoothly. The rupture propagation slowed down in the southwestern part of the fault. The rupture pattern is ambiguous in the southwestern part of the fault, because there are several solution which have equally small residuals but different rupture patterns in this area. However, the deceleration of rupture propagation and the relatively small slip at the shallowest part in the southwestern part of the fault are common features in these solutions. In Fig. 18, coseismic slip inferred from one of the inversion solutions is contoured at 0.75 m intervals with the distribution of accurately located aftershocks of magnitude grtater than 3

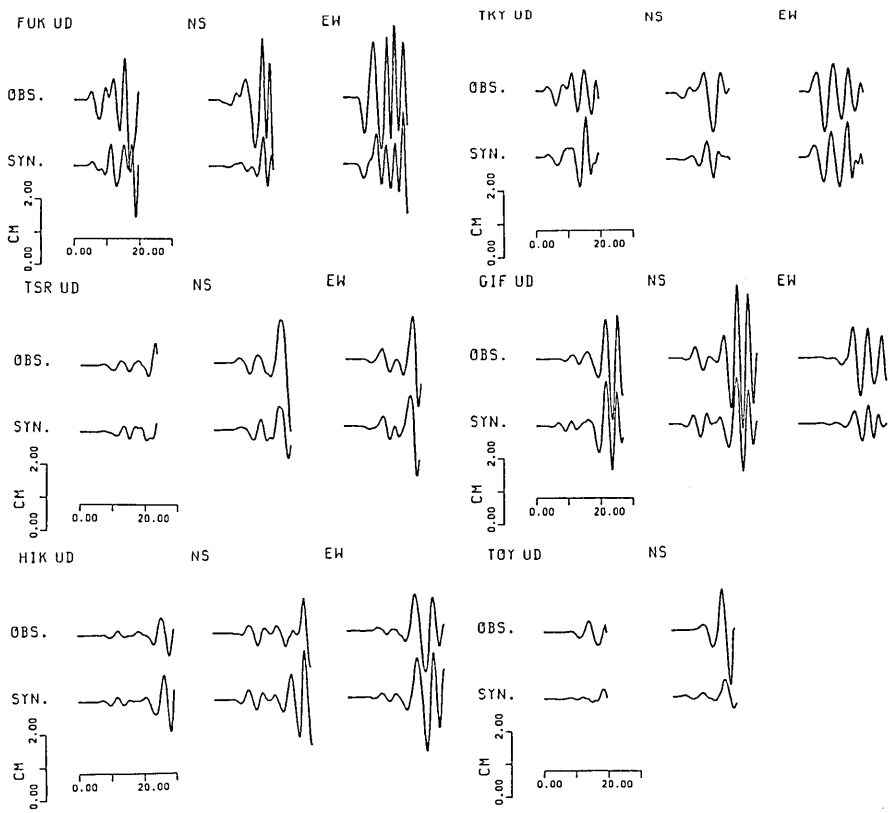

Fig. 13. Comparison of observed seismograms with synthetic seismograms obtained by using the solution for the 1961 Kitamino earthquake.

occurring in the first month after the main event (HAMADA, 1984). The rupture fronts at every second are shown in Fig. 17. The average slip on the whole fault and the total seismic moment are 0.9 m and 5×10^{25} dyne·cm, respectively. KAWASAKI (1975) determined the seismic moment of 9×10^{25} dyne·cm based on a leveling measurement which was made two or three months after the main event. The seismic moment determined from the strong motion records are smaller than Kawasaki's result. A

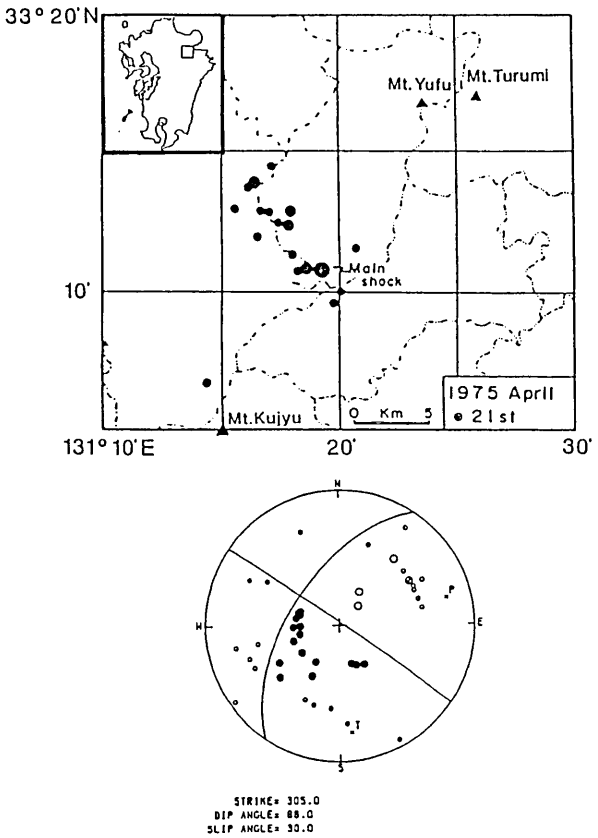

Fig. 14. Distribution of aftershocks of the OitaKen-Chubu earthquake which occurred at 0235JST on April 21, 1975 (MITSUNAMI and KUBOTERA, 1975). The aftershocks in this figure occurred on the day of the main event. The location of the source region is shown in the upper left corner. The focal mechanism of the main event obtained by HATANAKA and SHIMAZAKI (1988) is shown in the lower half of this figure. Solid and open circles in the focal mechanism indicate compressional and dilatational initial motions, respectively. The nodal plane striking SE-NW is inferred to be the fault plane from the distribution of the aftershocks [after HATA- NAKA and TAKEO (1989)].

possible explanation for the discrepancy is occurrence of quasi-static slip following the main event, but we don't have any data to confirm this speculation.

3.6. The 1975 OitaKen-Chubu earthquake

The OitaKen-Chubu earthquake of April 21, 1975, is the largest event (M=6.4) since 1941 in Kyusyu, Japan. HATANAKA and SHIMAZAKI (1988) and HATANAKA and TAKEO (1989) showed that this earthquake invelved left-lateral strike-slip motion on an almost vertical fault with a strike of N55°W. The focal mechanism (HATANAKA and SHIMAZAKI, 1988) and the distribution of aftershocks (MITSUNAMI and KUBOTERA, 1975) are indicated in Fig. 14. HATANAKA and TAKEO (1989) analyzed the detailed rupture process of this event using strong motion seismograms around the source region and teleseismic P-waves. They assumed a fault 10 km square divided into nine 3.3 km (length)×3.3 km (width) subfaults. The source duration of 3 sec was assumed for each subfault.

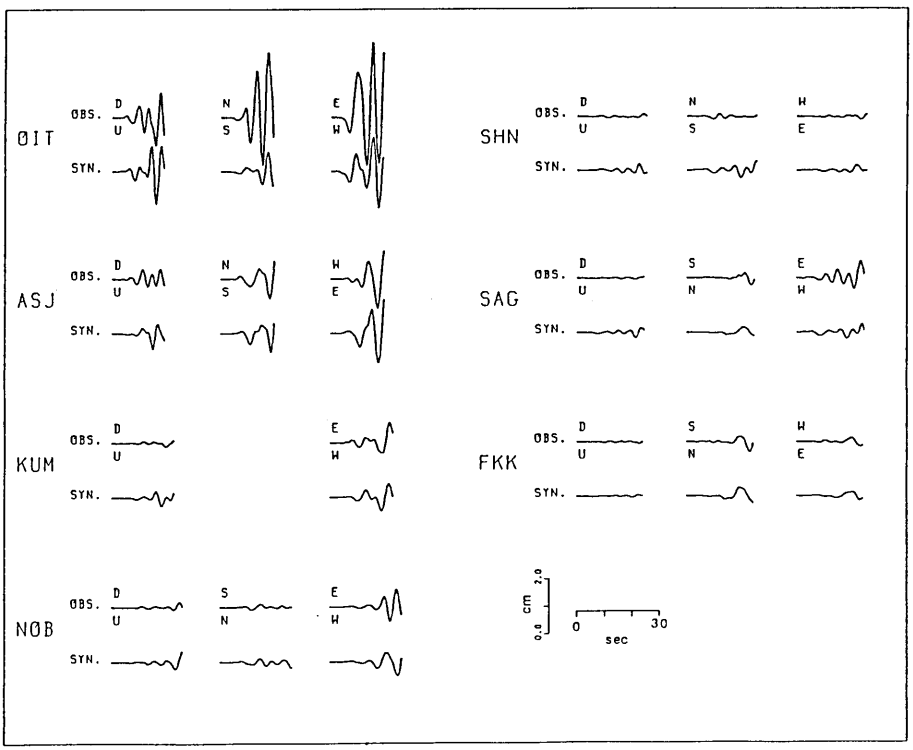

Fig. 15. Comparison of observed seismograms with synthetic seismograms obtained by using the solution for the 1975 OitaKen-Chubu earthquake [after HATANAKA and TAKEO (1989)].

The distribution of coseismic slip and the rupture fronts at every second are shown in Fig. 17. The observed strong motion seismograms and synthetic seismograms calculated for the inversion solution are shown in Fig. 15. The synthetics, especially, the amplitude ratio of different components, are consistent with the observations. In Fig. 16, teleseismic P-wave seismograms observed by WWSSN long-period seismographs are compared to synthetic seismograms calculated for the solution. Our source model can explain not only the near-field seismic waveforms but also the far-field waveforms.

A large slip occurred at the the deeper part of the fault; another relatively large slip occurred at the northwest end of the shallower part of the fault. The central part of the fault shows relatively little moment release, so the source process is divided into two subevents. The rupture

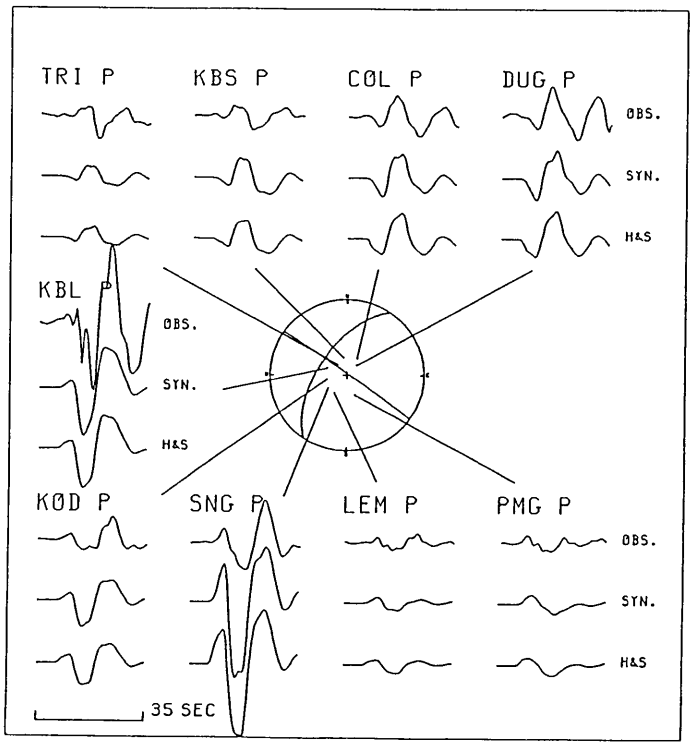

Fig. 16. Comparison of far-field P-wave seismograms (OBS) with synthetics calculated by using the parameters obtained in this study (SYN). The synthetic seismograms calculated by using a horizontal line source model after HATANAKA and SHIMAZAKI (1988) are shown in the bottom of the seismograms of each station (H&S). The observed records are the long-period WWSSN vertical component seismograms [after HATANAKA and TAKEO (1989)].

propagated from the southeast end of the deeper part to the northwest end of the shallower part of the fault. This rupture propagation suggests that the first event occurred at the deeper part of the fault and the second event at the northwest end of the shallower part of the fault. The total seismic moment is 3.4×10^{25} dyne·cm, and the average slip 1.3 m (HATANAKA and TAKEO, 1989).

4. Discussion

We compile all rupture processes of the six earthquakes in Fig. 17. The slip pattern, which is normalized with the average slip of the individual event, is represented in the left panel of each result. The rupture fronts at every second are shown in the right panel of each. The source parameters of the six earthquake are listed in Table 1. By comparing these results, it is recognized that the slip distributions of earthquakes with relatively smooth rupture propagation, such as the 1974 Izu-Hanto-Oki earthquake and the 1961 Kitamino earthquake, are smoother than those of earthquakes with relatively irregular rupture propagation, such as the 1969 GifuKen-Chubu earthquake and the 1980 Izu-Hanto-Toho-Oki earthquake.

In Fig. 18, each slip distribution is compared with the distribution of aftershocks. As the depths of aftershocks following the 1975 OitaKen-Chubu earthquake are not determined accurately, this earthquake is not shown in Fig. 18. All aftershocks of the 1974 Izu-Hanto-Oki earthquake are indicated with small dots because the magnitudes are not determined. Apparent in Fig. 18 is that aftershocks of magnitude greater than 4 do not occur in the large slip area during the main event; especially, you can confirm this clearly by the 1961 Kitamino earthquake, the 1969 GifuKen-Chubu earthquake, and the 1980 Izu-Hanto-Toho-Oki earthquake. Most large aftershocks took place near the edge of the large slip region and in the small slip region. Aftershocks also tend to cluster near the edge of the large slip region. Similar results are pointed out by DOSER and KANAMORI (1986), MENDOZA and HARTZELL (1988), and FUKUYAMA (1990) for other intraplate and interplate earthquakes which occurred in Japan and in North America. When nonuniform slip occurs on a fault plane due to heterogeneous prestresses and/or material strength, it is confirmed by numerical experiments of dynamic fault rupture that high stresses remain at areas where slip exhidits large gradient or small values, and that stresses are released in large slip areas (*e.g.*, MIKUMO and MIYATAKE, 1978). The

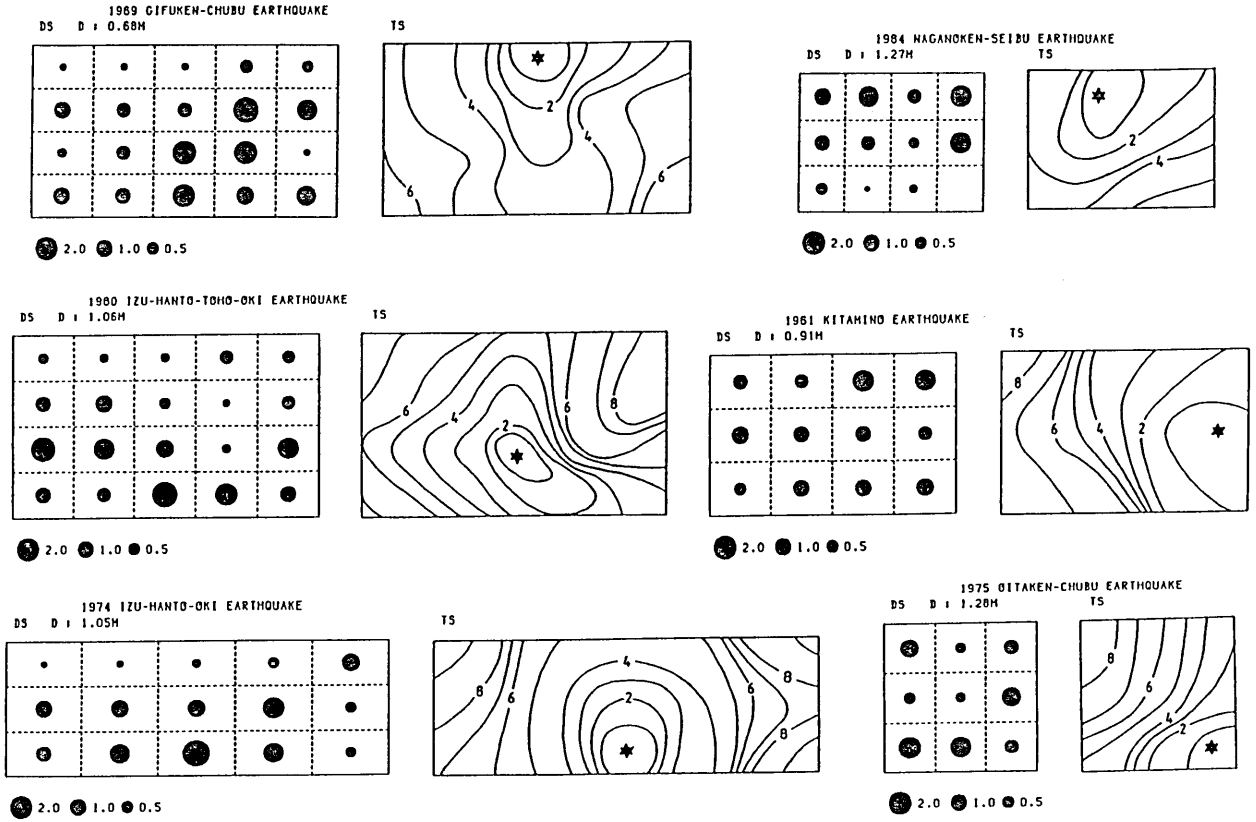

Fig. 17. Summary of the rupture processes of the six inland earthquakes. Each distribution of slip is normalized to each average slip whose value is shown above the left panel of each rupture process. The inferred rupture fronts of each earthquake are schematically illustrated in the right panel of each rupture process. Stars signify the central positions of subfaults where rupture initiated.

Table 1. Source parameters of earthquake.

The 1969 GifuKen-Chubu earthquake

Slip (m)

0.1	0.1	0.1	0.4	0.3
0.7	0.5	0.5	1.7	1.1
0.2	0.5	1.5	1.4	0.1
0.7	0.6	1.3	0.8	1.0

Time (sec)

4.25	3.00	0.00	1.75	3.75
4.25	3.75	1.50	4.00	5.50
4.75	4.50	2.25	3.50	5.00
5.50	4.00	3.25	3.50	6.00

The 1980 Izu-Hanto-Toho-Oki earthquake

Slip (m)

0.4	0.3	0.3	0.7	0.6
0.9	1.2	0.5	0.2	0.7
2.6	1.9	1.3	0.3	1.8
1.0	0.8	2.7	2.0	1.0

Time (sec)

6.00	5.75	3.00	5.50	6.75
6.25	3.75	2.75	5.50	8.00
4.50	2.50	0.00	5.75	5.25
6.25	3.50	1.50	1.25	3.00

The 1974 Izu-Hanto-Oki earthquake

Slip (m)

0.1	0.2	0.3	0.5	1.3
1.2	1.2	1.2	1.8	0.4
1.0	1.6	3.0	1.7	0.4

Time (sec)

8.50	4.00	3.50	4.00	8.00
7.00	3.50	1.50	2.50	6.00
6.00	3.50	0.00	3.00	8.50

The 1984 NaganoKen-Seibu earthquake

Slip (m)

1.3	2.0	0.9	2.2
1.1	0.9	0.5	2.2
−0.6	−0.1	0.3	0.0

Time (sec)

2.00	0.00	0.75	1.00
1.50	0.75	1.75	2.75
		4.25	

The 1961 Kitamino earthquake

Slip (m)

0.7	0.6	1.6	1.5
1.0	0.8	0.8	0.6
0.5	0.9	0.9	1.0

Time (sec)

7.75	3.00	2.00	1.25
5.25	3.50	0.75	0.00
7.00	6.00	1.50	0.75

The 1975 OitaKen-Chubu earthquake

Slip (m)

1.6	0.5	1.0
0.6	0.4	1.7
2.5	2.3	0.9

Time (sec)

7.25	5.50	3.00
6.75	4.75	2.25
4.50	1.25	0.00

aftershock patterns are very consistent with the results of numerical experiments, so it is suggested that the relation between aftershocks and coseismic slip pattern is general feature for an earthquake rupture process.

There is a clear contradiction between the rupture processes of the 1969 GifuKen-Chubu earthquake and of the 1980 Izu-Hanto-Toho-Oki earthquake. The large slip area northwest of and below the hypocenter during the 1969 GifuKen-Chubu earthquake shows deceleration of rupture propagation. On the other hand, the area north of the hypocenter of the 1980 Izu-Hanto-Toho-Oki earthquake is characterized by small slip and deceleration of rupture propagation, and large slip areas greater than 2 m show relatively fast rupture propagation.

According to numerical experiments of dynamic rupture (*e.g.*, MIKUMO and MIYATAKE, 1978; MIYATAKE, 1980; DAS, 1981; DAY, 1982; MIKUMO *et al.*, 1987), the large slip area during the 1969 GifuKen-Chubu earthquake might have a high frictional strength and suffer lower initial shear stress enough to act as a barrier in the initial stage of the rupture progress. After a few seconds from the start of rupture, the shear stress in the area might exceed the frictional strength; the area is broken with a high stress drop which produces the large slip.

On the contrary, the physical background of the rupture process of the 1980 Izu-Hanto-Toho-Oki earthquake seems to be complicated. Many young

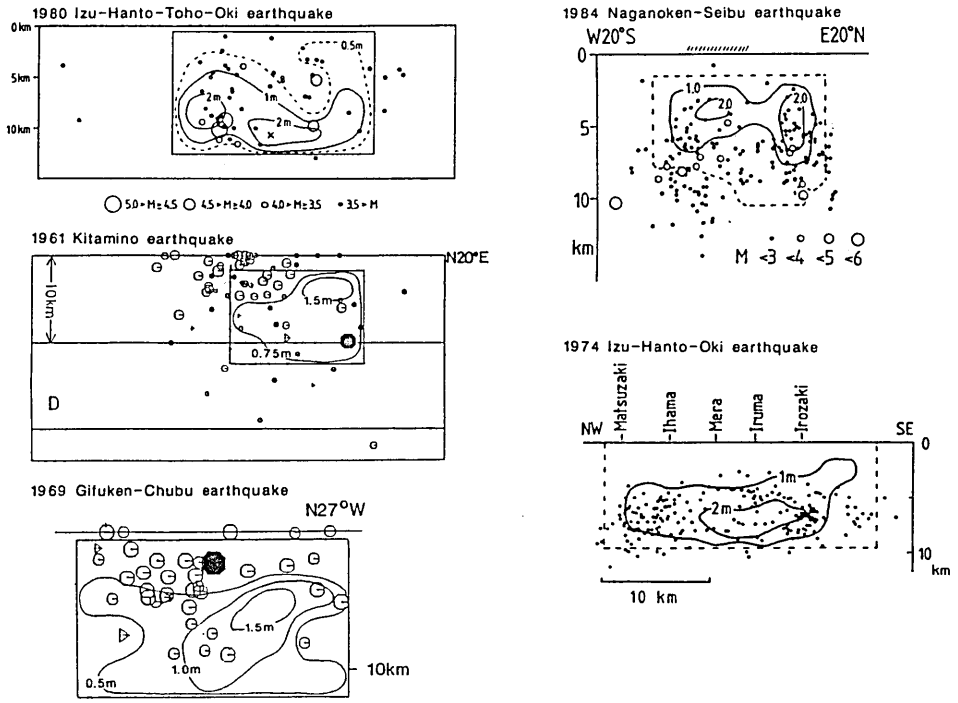

Fig. 18. Slip distribution and hypocenter of aftershocks. Isograms of the slip inferred from the solution are drawn with solid and/or broken lines on the fault plane. In case of the 1984 NaganoKen-Seibu earthquake, the broken lines denote the edge of the fault plane obtained from the slip distribution. In the hatched area of the 1984 NaganoKen-Seibu earthquake, high accelerations in excess of 1G are estimated from field investigations. As the magnitudes of aftershocks of the 1974 Izu-Hanto-Oki earthquake are not determined, these aftershocks are indicated with small dots. In some cases, small aftershocks have occurred in the large slipped area; however, aftershocks of magnitude greater than 4 do not occur in the large slip area. This characteristic is common to all these rupture processes. Most large aftershocks take place in areas where the slip gradient is large, or a small slip occurs during the main event where high stresses are expected to remain after the main event's faulting.

and small submarine volcanoes have been identified in the region between the eastern coast of the Izu Peninsula and Oshima island (HAMURO *et al.*, 1980, 1983). The small submarine monogenetic volcanoes located above the source region are represented by shaded areas in the submarine topography of Fig. 19. Comparing the slip pattern with the distribution of the submarine volcanoes, it is recognized that the shallower fault levels beneath the volcanoes is characterized by small slip and deceleration of rupture propagation, and the large slip areas with first rupture propagation are located at deeper fault levels beneath the volcanoes.

A possible explanation for this non-uniform rupture process is that volcanoes are mechanical weak spots in the Earth's crust (NAKAMURA, 1987).

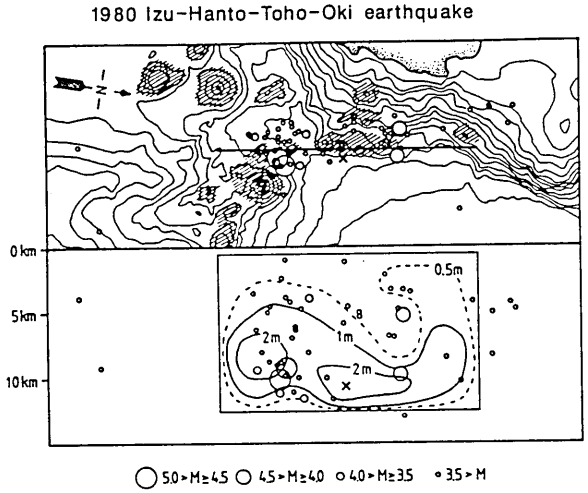

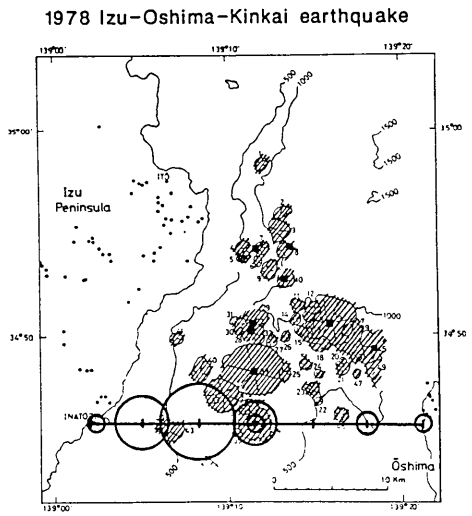

(after Kikuchi and Sudo, 1984)

Fig. 19. A heterogeneous rupture process of the 1980 Izu-Hanto-Toho-Oki earthqake related to the geological structure in the source region (same scheme as Fig. 3). In the lower panel is illustrated the subevents location of the 1978 Izu-Oshima-Kinkai earthquake which occurred about 10 km south of the 1980 Izu-Hanto-Toho-Oki earthquake. These subevents were determined by KIKUCHI and SUDO (1984) using far-field P-wave seismograms.

Because of their weakness, relatively ductile areas begin to aseismically deform earlier than relatively brittle, surrounding regions. This deformation creates high stress areas in the relatively brittle regions which adjoin to the volcanoes and low stress areas within the relatively ductile volcanoes (NAKAMMRA, 1987). According to numerical simulations of dynamic shear crack spreading (*e.g.*, MIKUMO and MIKATAKE, 1978; MIYATAKE, 1980; DAS, 1981; DAY, 1982; MIKUMO *et al.*, 1987), it seems reasonable that a high prestress area experiences large slip and fast rupture propagation during the rupture progress, and a low prestress area experiences small slip and deceleration of rupture propagation. It is not clear how large the low stress area is in the submarine volcanoes located above the source region of the largest event. However, swarm events that preceded the largest event were concentrated at the northern end of the large slip area near the hypocenter (MATSU'URA, 1983). Therefore, it seems possible that relatively brittle media exist in regions deeper than several kilometers beneath the submarine volcanoes. In these relatively brittle regions, the areas adjacent to the submarine volcanoes might correspond to high prestress areas and act as asperities during the event's faulting. The area characterized by small slip and deceleration of rupture propagation seems to correspond to the low prestress area in the submarine volcanoes.

In the lower panel of Fig. 19 is illustrated the subevent locations of the 1978 Izu-Oshima-Kinkai earthquake which occurred about 10 km south of the 1980 Izu-Hanto-Toho-Oki earthquake, These subevents were determined by KIKUCHI and SUDO (1984) using teleseismic P-wave seismograms. The large subevents occur near the submarine monogenetic volcanoes: this suggests that a similar geological condition also affects the rupture process of the 1978 Izu-Oshima-Kinkai earthquake.

5. Conclusions

Detailed rupture processes of six intraplate earthquakes in Japan inferred from waveform inversion analysis using strong motion seismograms are compiled and compared to each other in this paper to make clear common features of the earthquake rupture process. Five of these rupture processes are also compared with the distribution of aftershocks.

It is recognized that earthquakes with relatively smooth rupture propagation have smoother slip distribution than earthquakes with relatively irregular rupture propagation. Also apparent in the comparison is that aftershocks of magnitude greater than 4 do not occur in the large slip area during the main event. Most large aftershocks take place near the edge of

the large slip region and in the small slip region. Aftershocks also tend to cluster near the edge of the large slip region. Aftershock patterns are consistent with the results of numerical experiments, so it is suggested that the relation between aftershocks and coseismic slip pattern mentioned above is a general feature of an earthquake rupture process.

There is a contradiction between the rupture processes of the 1969 GifuKen-Chubu earthquake and the 1980 Izu-Hanto-Toho-Oki earthquake. A clear delay of rupture propagation occurs in the large slip area during the 1969 GifuKen-Chubu earthquake, on the other hand, the small slip area in the 1980 Izu-Hanto-Toho-Oki earthquake is characterized by deceleration of rupture propagation. The large slip area in the former case is interpreted as a barrier which resisted fracturing in the first stage of the rupture progress and was broken with a high stress drop. In the later case, the mechanical weakness of volcanoes, located around the source region, seems to have affected the rupture process.

Acknowledgments

The authors express their gratitude to the staff of the JMA (Japan Meteorological Agency) stations for supplying the strong motion seismograms. The inversion program SALS (Statisoical Analysis with Least-Squares fitting) was used in this study. The numerical computations were implemented on a HITAC M-280H computer at the Earthquake Research Institute, University of Tokyo.

References

BOUCHON, M., 1981, A simple method to calculate Green's functions for elastic layered media, *Bull. Seism. Soc.. Amer.*, 71, 959-971.

DAS, S., 1981, Three-dimensional spontaneous rupture propagation and implications for the earthquake source mechanism, *Geophys. J.R. Astr. Soc.* 67, 375-393.

DAY, S.M., 1982, Three-dimensional simulation of spontaneous rupture: The effect of nonuniform prestress, *Bull. Seism. Soc. Amer.*, 72 1881-1902.

DOSER, D.I. and H. KANAMORI, 1986, Depth of seismicity in the Imperial Valley region (1977-1983) and its relationship to heat flow, crustal structure, and the October 15, 1979, earthquake, *J. Geophys. Res.*, 91, 675-688.

FUKUYAMA, E., 1990, Analysis and interpretation of heterogeneous rupture process: Application of EGF method and nonlinear inversion technique to large earthquakes, *Tectonophysics*, (submitted).

FUKUYAMA, E. and K. IRIKURA, 1986, Rupture process of the 1983 Japan Sea (Akita-Oki) earthquake using a waveform inversion method, *Bull. Seism. Soc. Amer.*, 76, 1923-1640.

HAMADA, N., 1984, Reexamination of aftershock distribution and seismic activity associated with inland earthquakes, Japan, *Program and Abstracts, Seism. Soc. Japan,*

1, 75.

HAMURO, K., S. ARAMAKI, H. KAGAMI and K. FUJIOKA, 1980, The Higashi-Izu-oki submarine volcanoes, Part 1, *Bull. Earthq. Res. Inst., Tokyo Univ.*, 55, 259-297.

HAMURO, K., S. ARAMAKI, K. FUJIOKA, T. ISHII, T. TANAKA and K. UTO, 1983, The Higashi-Izu-oki submarine volcanoes, Part 2, and the submarine volcanoes near the Izu Shoto Islands, *Bull. Earthq. Res. Inst., Tokyo Univ.*, 58, 527-557.

HATANAKA, Y. and K. SHIMAZAKI, 1988, Rupture process of the 1975 central Oita, Kyushu, Japan, earthquake, *J. Phys. Earth.*, 36, 1-15.

HATANAKA, Y. and M. TAKEO, 1989, Detailed rupture process of the 1975 central Oita, Japan, earthquake inferred from near-field data, *J. Phys. Earth.*, 37, 251-264.

HARTZELL, S.H. and T.H. HEATON, 1983, Inversion of strong ground motion and teleseismic waveform data for the fault rupture history of the 1979 Imperial Valley, California, earthquake, *Bull. Seism. Soc. Amer.*, 73, 1553-1583.

HYDROGRAPHIC DEPARTMENT, MARITIME SAFETY AGENCY, 1977, Submarine topography and geological structure off east coast of Izu-Peninsula (Preliminary Report), *Rep. Coord. Comm. Earthq. Predict.*, 18, 64-67.

ISHIBASHI, K., K. SUEHIRO, E. INATANI, T. MATSUZAKI and T. ASADA, 1975, Hight gain observation of the aftershocks of the Izu-Hanto-Oki earthquake of 1974, *The Report of the Investigations and Studies about the Activity and Damages of the 1974 Izu-Hanto-Oki Earthquake*. pp. 21-26.

JAPAN METEOROLOGICAL AGENCY, 1986, Report on the NaganoKen-Seibu earthquake, 1984, *Tech. Rep. Japan Meteorol. Agency*, 107, 1-46.

KARAKAMA, I., K. TSUMURA, M. TAKAHASHI, I. OGINO and K. SAKAI, 1974, Observation of the aftershocks of the Izu-Hanto-Oki earthquake of 1974, *Spec. Bull. Earthq. Res. Inst., Univ. Tokyo*, 14, 55-67.

KAWASAKI, I., 1975, The focal process of the Kita-Mino earthquake of August 19, 1961, and its relationship to a quaternary fault, the Hatogayu-Koike fault, *J. Phys. Earth*, 24, 227-250.

KENNETT, L.N. and N.J. KERRY, 1979, Seismic waves in a stratified half space, *Geophys. J.R. Astr. Soc.*, 57, 557-583.

KIKUCHI, M. and Y. FUKAO, 1985, Iterative deconvolution of complex body waves from great eathquakes—the Tokachi-Oki earthquake of 1968, *Phys. Earth Planet. Inter.*, 37, 235-248.

KIKUCHI, M. and K. SUDO, 1984, Inversion of teleseismic P waves of Izu-Oshima, Japan earthquake of January 14, 1978, *J. Phys. Earth*, 32, 161-171.

MATSUDA, T. and K. YAMASHINA, 1974, Surface faults associated with the Izu-Hanto-Oki earthquake of 1974, Japan, *Spec. Bull. Earthq. Res. Inst., Univ. Tokyo*, 14, 135-158.

MATSU'URA, R.S., 1983, Detailed study of the earthquake sequence in 1980 off the east coast of the Izu Peninsula, Japan, *J. Phys. Earth*, 31, 65-101.

MENDOZA, C. and S.H. HARTZELL, 1988, Aftershock patterns and main shock faulting, *Bull. Seism. Soc. Amer.*, 78, 1438-1449.

MIKAMI, N. aud M. TAKEO, 1987, Rupture process of the 1961 Kitamino earthquake, *Program and Abstracts, Seism. Soc. Japan*, 2, 242.

MIKAMI, N. and M. TAKEO, 1990, Rupture process of the 1969 GifuKen-Chubu earthquake, *Bull. Seism. Soc. Japan*, (in preparation).

MIKUMO, T., 1973, Faulting mechanism of the Gifu earthquake of September 9, 1969 and some related problems, *J. Phys. Earth*, 21, 191-212.

MIKUMO, T. and T. MIYATAKE, 1978, Dynamical rupture process on a three-dimensional fault with non-uniform frictions and near-field seismic waves, *Geophys. J.R. Astr. Soc.*, 54, 417-438.

MIKUMO, T., K. HIRAHARA and T. MIYATAKE, 1987, Dynamical fault rupture processes in heterogeneous media, *Tectonophysics*, 144, 19-36.

MITSUNAMI, T. and A. KUBOTERA, 1975, Seismicity of the central part of Oita earthquake, in *The Report of the Investigations and Studies about the Activity and Damages of the 1975 Central Part of Oita Earthquake*, edited by I. UCHIDA, pp. 2-14, Ministry of Education, Science and Culture.

MIYATAKE, T., 1980, Numerical simulations of earthquake source process by a three-dimensional crack model, Part 1, rupture process, *J. Phys. Earth*, 28, 565-598.

MORI, J. and K. SHIMAZAKI, 1985, Inversion of intermediate-period Rayleigh waves for source characteristics of the 1968 Tokachi-Oki earthquake, *J. Geophys. Res.*, 90, 11374-11382.

NAKAMURA, K., 1987, Volcanoes as mechanically weak spots in the crust, with special reference to the 1986 eruption of Izu-Oshima volcano, *Proc. Earthq. Predict. Symp.*, 237-241.

OLSON, A.H., 1982, Forward simulation and linear inversion of earthquake ground motion, *Ph. D thesis, Univ. California, San Diego.*

TAKEO, M., 1985, Near-field synthetic seismograms taking into account the effects of anelasticity—The effects of anelastic attenuation on seismograms caused by a sedimentary layer—, *Meteorol. Geophys.*, 36, 245-257.

TAKEO, M., 1987, An inversion method to analyze the rupture processes of earthquakes using near-field seismograms, *Bull. Seism. Soc. Amer.* 77, 490-513.

TAKEO, M., 1988, Rupture process of the 1980 Izu-Hanto-Toho-Oki earthquake deduced from strong motion seismograms, *Bull. Seism. Soc. Amer.*, 78, 1074-1091.

TAKEO, M., 1989, Rupture process of the 1974 Izu-Hanto-Oki earthquake, *Bull. Selsm. Soc. Japan*, 42, 59-66.

TAKEO, M. and N. MIKAMI, 1987, Inversion of strong motion seismograms for the source process of the NaganoKen-Seibu earthquake of 1984, *Tectonophysics*, 144, 271-285.

日本内陸地震の不均質な断層活動

東京大学地震研究所　武尾　実
気象庁松代地震観測所　三上直也

日本内陸で発生した6つの地震について，詳細な破壊過程を取りまとめ，それらの相互の特徴及び余震分布との対応等を調べた．取り上げた地震は1961年北美濃地震・1969年岐阜県中部地震・1974年伊豆半島沖地震・1975年大分県中部地震・1980年伊豆半島東方沖地震及び1984年長野県西部地震である．これらの地震については，震源近くで記録された強震計記録の波形インバージョンにより，詳細な破壊過程が解明されている．

比較的，断層面上でのすべりの分布が滑らかな地震の場合には，その破壊伝播も滑らかであるが，すべり分布が不均質な地震では破壊の進行もあまり滑かではない．また，マグニチュード4以上の比較的大きな地震は，本震時には大きくすべった領域では発生しておらず，本震時のすべり量の変化の大きな領域やあまりすべらなかった領域に大きな余震が発生する傾向がみられる．この様な特徴は，動的な断層破壊のシュミレーションから推定される結果とも調和的であり，地震の断層運動の一般的特徴といえる．

1969年岐阜県中部地震と1980年伊豆半島東方沖地震の破壊過程には相反する様子がみられる．前者では，大きいすべりを起こした領域の破壊はやや遅れて発生しているのに対し，後者では，破壊伝播の遅れがみられる領域ではほとんどすべりを起していない．前者の場合は，バリアーがやや遅れて破壊したものと解釈される．後者の場合は，震源域付近にある単成火山群が力学的弱点であることが地震の破壊過程に影響を与えたものと考えられる．